

# Structural Features of a Hyperthermostable Endo- $\beta$ -1,3-glucanase in Solution and Adsorbed on “Invisible” Particles

Sotirios Koutsopoulos,\* John van der Oost,<sup>†</sup> and Willem Norde\*<sup>‡</sup>

\*Laboratory of Physical Chemistry and Colloid Science, and <sup>†</sup>Laboratory of Microbiology, Wageningen University, Wageningen, The Netherlands; and <sup>‡</sup>Department of Biomedical Engineering, University of Groningen, Groningen, The Netherlands

**ABSTRACT** Conformational characteristics and the adsorption behavior of endo- $\beta$ -1,3-glucanase from the hyperthermophilic microorganism *Pyrococcus furiosus* were studied by circular dichroism, steady-state and time-resolved fluorescence spectroscopy, and calorimetry in solution and in the adsorbed state. The adsorption isotherms were determined on two types of surfaces: hydrophobic Teflon and hydrophilic silica particles were specially designed so that they do not interact with light and therefore do not interfere with spectroscopic measurements. We present the most straightforward method to study structural features of adsorbed macromolecules in situ using common spectroscopic techniques. The enzyme was irreversibly adsorbed and immobilized in the adsorbed state even at high temperatures. Adsorption offered further stabilization to the heat-stable enzyme and in the case of adsorption on Teflon its denaturation temperature was measured at 133°C, i.e., the highest experimentally determined for a protein. The maintenance of the active conformation and biological function particularly at high temperatures is important for applications in biocatalysis and biotechnology. With this study we also suggest that nature may employ adsorption as a complementary mode to maintain structural integrity of essential biomolecules at extreme conditions of temperature.

## INTRODUCTION

Nature has developed adaptation mechanisms to maintain life in extreme environments such as volcanic areas and submarine hydrothermal vents. Hyperthermophilic microorganisms belonging to the archaea thrive at conditions of extreme temperature (60–120°C) (Brown and Doolittle, 1997). Hyperthermostable proteins from such microorganisms have attracted research interest owing not only to important applications but also because they are stable and biologically active under conditions that were previously regarded as incompatible with life (Rothschild and Mancinelli, 2001). LamA is an endo- $\beta$ -1,3-glucanase from the hyperthermophilic *Pyrococcus furiosus* that hydrolyzes polysaccharides and selectively attacks 1,3- $\beta$ -glucosyl bonds (Gueguen et al., 1997; Driskill et al., 1999). It is the most stable endoglucanase reported until now and displays maximum enzymatic activity at 104°C with substantial thermal stability.

The interaction of proteins with surfaces often leads to adsorption, i.e., excess accumulation of the protein molecules at the interface. This has important applications in protein chromatography, immunoassays for medical diagnostic tests, development of biosensors, biotechnology, and biocatalysis (Bowers and Carr, 1980; Scouten, 1983). Many of the enzymes used to date are obtained from mesophilic organisms but when the use of high temperatures is a prerequisite then the methodology to improve their

properties is based on directed mutation or DNA shuffling (Cherry et al., 1999; Lehmann et al., 2000). However, even the best performing mutants of mesophilic enzymes have inferior heat stability properties as compared to the respective extremophiles that moreover, are excellent candidates for mutation with further improved features.

Therefore, it is essential to analyze the structural characteristics of the surface-bound hyperthermophilic LamA and assess its performance for the enzymatic reaction catalyzed. To investigate the adsorption process two types of surfaces were selected: hydrophobic Teflon and hydrophilic silica. The sorbent particles were specially designed so that they do not interact with light when dispersed in dilute suspensions and, hence, are “invisible” to spectroscopic techniques that monitor only the protein features. We will focus on the adsorption of the extremely heat-stable LamA emphasizing structural characteristics and enzymatic activity in the adsorbed state. Heat-resilient features of the enzyme adsorbed at the solid/liquid interface will be compared with those in the dissolved state.

## MATERIALS AND METHODS

### The enzyme

Overproduction and purification of recombinant LamA (sequence deposited in the GenBank database: accession No. AF013169) cloned in *Escherichia coli* was done according to a method described in literature (Gueguen et al., 1997). The *E. coli* cells were transfected with BL21 plasmid vector harboring the cDNA for LamA and cloned into pGEF+ under control of the T7 promoter (Rink et al., 1997; Studier et al., 1990). The molecular mass of LamA is 30,085 Da and its isoelectric point is 4.4 as determined by MALDI-TOF mass spectroscopy and isoelectric focusing, respectively. The enzyme

Submitted March 22, 2004, and accepted for publication October 4, 2004.

Address reprint requests to Sotirios Koutsopoulos, Laboratory of Physical Chemistry & Colloid Science, Wageningen University, PO Box 8038, 6700 EK Wageningen, The Netherlands. Tel.: +31-317-482178; Fax: +31-317-483777; E-mail: sotiris.koutsopoulos@wur.nl.

© 2005 by the Biophysical Society

0006-3495/05/01/467/08 \$2.00

doi: 10.1529/biophysj.104.043323

was stored in 0.01 M sodium phosphate buffer at pH 7.0, free of antimicrobial agents (e.g., azide), which may affect the adsorption process.

## The sorbents

Negatively charged hydrophobic Teflon particles were supplied as a colloidal suspension (Dupont de Nemours, Le Grand-Saconnex, Switzerland). Monodispersity was confirmed by dynamic light scattering (DLS) and transmission electron microscopy (TEM) (JEOL 1200 EX). From these data the particle diameter was calculated (215 nm). The specific surface area is  $22.5 \text{ m}^2/\text{g}$  as determined by the B.E.T. method. Electrokinetic measurements showed that the particles are negatively charged. The hydrophobicity of Teflon was evidenced by contact angle measurements of a sessile water droplet on pelletized particles. The analysis revealed a contact angle of  $96^\circ$ .

Negatively charged silica nanoparticles (Ludox HS-40; Sigma-Aldrich, St. Louis, MO) were monodisperse as confirmed by DLS measurements. The particles are nonporous, smooth spheres with a specific surface area of  $220 \text{ m}^2/\text{g}$  and their average diameter is 13 nm as shown from TEM analysis. At the experimental conditions employed, the surface of silica is negatively charged (point of zero charge (p.z.c.) was at pH 2.7) and highly hydrophilic; water droplets spread on the surface with a contact angle  $<5^\circ$ .

The particles used are specially designed to study the structural characteristics of LamA in the adsorbed state using standard spectroscopic techniques. The refractive index of suspended Teflon particles is 1.35, which is close to the respective value of water (1.33) and is free of ultraviolet (UV)-absorbing groups. Hence, a low concentration dispersion of the enzyme-covered Teflon particles can be directly used for circular dichroism and fluorescence measurements without interference with light. On the other hand, the extremely small size of the ultrafine silica nanoparticles allows for negligible scattering of light by a highly dispersed particle suspension that, moreover, is characterized by large area/volume ratio enabling high protein concentrations in the adsorbed state.

## Adsorption experiments

All adsorption experiments were performed in Eppendorf tubes that were previously tested and did not give adsorption of LamA. Each tube contained different LamA concentrations in 0.01 M sodium phosphate at pH 7.0 and the same sorbent surface area to give a series of samples with the same total volume. The samples were incubated end-over-end overnight at room temperature. Preliminary experiments showed that in this period of time, adsorption reached a steady state. The enzyme-covered particles were removed from the suspension by centrifugation. The concentration of LamA in the supernatant was measured with a spectrophotometer from the absorption peak at 280 nm (the experimentally determined extinction coefficient is  $\epsilon_{280} = 3.08 \text{ L g}^{-1} \text{ cm}^{-1}$ , for 1-cm cell) and with the Bradford assay (Bradford, 1976). The adsorbed amount per unit surface area,  $\Gamma$ , was calculated from the difference of the protein concentration in solution before and after adsorption,  $c_{\text{eq}}$ , using mass balance considerations and the sorbent's specific surface area. All data points in the adsorption isotherm represent an average of three experiments. After separation from the supernatant the enzyme-covered particles were redispersed in the original buffer and used for further analyses. Immobilization of LamA in the adsorbed state was tested by overnight incubation of the redispersed enzyme-covered particles at room temperature, for 5 h at  $90^\circ\text{C}$  and for 1 h at  $100^\circ\text{C}$ .

## Enzymatic activity measurements

The enzymatic activity of LamA free in solution and in the adsorbed state was measured for 10 min at  $90^\circ\text{C}$  using the DNS (3,5-dinitrosalicylic acid) assay (Miller, 1959). This method is based on the spectrophotometric determination of the amount of hydrolyzed ends carried by the oligosaccharides resulting from degradation of the substrate (i.e., laminarin). The Michaelis-Menten constant,  $K_m$ , of LamA for the hydrolysis of laminarin is  $2.8 \text{ mg/ml}$  (Gueguen et al., 1997). To test whether adsorption affected  $K_m$ ,

the enzymatic activities were measured using a range of 0.5–100 mg of substrate/mL. The specific enzymatic activities of LamA were then compared to assess the effect of adsorption on the activity.

## Circular dichroism

Circular dichroism (CD) spectroscopy was used to examine the secondary structure of LamA free in solution and adsorbed on Teflon and silica. Far-UV CD spectra of 0.25 mg/mL LamA were recorded in a J-715 (Jasco, Tokyo, Japan) spectrophotometer in 0.1-cm pathlength quartz cuvettes in the temperature range  $20\text{--}90^\circ\text{C}$ . Spectral analysis was performed by fitting the spectra acquired (between 190 and 260 nm) with reference spectra using the CONTIN software, which is based on nonlinear regression algorithms without constraints (ridge-regression analysis) (Venyaminov et al., 1993; Provencher and Glöckner, 1981), and gives better estimate of  $\beta$ -structures than simple multiple linear regression (Greenfield, 1996).

## Fluorescence emission spectroscopy

Emission steady-state fluorescence was measured between 20 and  $90^\circ\text{C}$  by a Varian Cary Eclipse spectrophotometer (Palo Alto, CA). Fluorescence spectra of 0.025 mg/mL LamA in solution and adsorbed on Teflon or silica were recorded between 300–400 nm on excitation at 300 nm in a quartz cuvette of 1-cm pathlength. All spectra were corrected for the background emission of water.

## Time-resolved fluorescence and anisotropy

Time-correlated single-photon counting was used to detect polarized time-resolved fluorescence and anisotropy on the subnanosecond timescale. Details on the setup and the method are described elsewhere (van den Berg et al., 1998; Visser et al., 1998). A CW diode-pumped, frequency-doubled Nd:YVO<sub>4</sub> laser was used with pulse duration of 3 ps full width half-maximum at 295 nm and maximum pulse energy a few pJ. A combination of polarizers, interference filters, and lenses was used between light source, sample, and photomultiplier to avoid artifacts from depolarization and misalignment. The fluorescence was collected at an angle of  $90^\circ$  with respect to the excitation light beam. The data were collected in 4096 channels of a multichannel analyzer with 11.1-ps channel width. Data analysis of the time-resolved fluorescence intensity  $I(t)$  and anisotropy  $r(t)$  decays was done with a program that performed global analysis over the emission spectrum at different time windows and employed a reweighted iterative deconvolution method (Novikov et al., 1999; Digris et al., 1999). Optimal fit was judged by the value of the parameter,  $\chi^2$ , which was close to unity, and inspection of the weighted residuals and autocorrelation function graphs that were uniformly distributed around zero. From the fitting, a set of fluorescence and rotational lifetimes,  $\tau_i$  and  $\phi_i$ , with amplitudes  $\alpha_i$  and  $\beta_i$ , were obtained for the fluorescence and anisotropy decays, respectively. The weighted average fluorescence lifetime  $\langle\tau\rangle$  was calculated from the lifetime spectrum  $\alpha(\tau)$ .

## Differential scanning calorimetry

Differential scanning calorimetric (DSC) studies were carried out in a recently constructed high-temperature MC-DSC 4100 calorimeter (Calorimetry Sciences Corp., Lindon, UT) with scanning temperature efficiency up to  $200^\circ\text{C}$ . Dissolved LamA or the suspension with the enzyme-covered particles was placed into 1 mL cells using as reference the buffer solution or the sorbent dispersion without adsorbed enzyme, respectively. Very small heat exchanges were measured upon heating the samples with scan rate of  $1^\circ\text{C}/\text{min}$ .

## RESULTS

LamA is a single domain globular-ellipsoid protein with dimensions  $4.6 \times 3.2 \times 3.4 \text{ nm}$  as calculated using a

simulation software (Combet et al., 2002), and the atomic coordinates of an endoglucanase from *Bacillus licheniformis* with high sequence identity (Hahn et al., 1995). Spectroscopic data from this work and structural analysis from preliminary NMR data were used for the selection of the best model. The enzyme in solution is a monomer as pointed out by dynamic-light-scattering studies.

### Adsorption isotherms

Fig. 1 shows the adsorption isotherms for LamA on negatively charged hydrophobic Teflon latex and hydrophilic silica nanoparticles. The protein surface concentration ( $\Gamma$ ) is plotted as a function of the concentration in solution ( $c_{eq}$ ) after adsorption reached a steady state. Adsorption isotherms showed well-defined plateau values that are different for the two surfaces. Electrostatic repulsions were not sufficient to preclude adsorption of the negatively charged LamA at pH 7.0 on the negatively charged Teflon and silica particles. Comparison of the adsorption isotherms shows that the hydrophobic surface attracts significantly more enzyme molecules than the hydrophilic silica. The maximum surface concentration of LamA on Teflon and silica was found to be 1.9 mg/m<sup>2</sup> and 0.82 mg/m<sup>2</sup>, respectively. Assuming that the adsorbed molecules form a monolayer and do not change their conformation upon adsorption, then using the molecular dimensions of native LamA surrounded by a hydration layer of 0.23-nm thickness, the surface coverage is calculated 78% and 34% for the Teflon and silica particles, respectively. The relatively low surface coverage on silica may be attributed to the significance of electrostatic interactions upon adsorption.

### Desorption tests

Redispersion and dilution of the enzyme-covered particles in the original solvent did not result in detectable changes in the surface concentration of LamA. Even after heat treatment for 5 h at 90°C and for 1 h at 100°C desorption of LamA barely occurred. This suggests irreversible adsorption although

a hysteresis effect upon desorption cannot be excluded (i.e., slow desorption at longer times).

### Enzymatic activity tests

The specific enzymatic activity of LamA in solution was ca. 1545 units/mg at 90°C. Samples of adsorbed LamA were selected from the middle of the adsorption isotherm (fifth point of the isotherms presented in Fig. 1) and from the plateau that represents adsorption saturation. As may be seen in Fig. 2, LamA in the adsorbed state remains biologically active but the specific activity is decreased to ~50% relative to that for the enzyme in solution. In all cases, the  $K_m$  constants of LamA in solution and in the adsorbed state were the same and, therefore, we can conclude that the decreased activity is not due to major structural alterations of the enzyme upon binding to the adsorbents.

### Circular dichroism

The secondary structure of LamA in solution and immobilized on the surface of Teflon and silica was determined using far-UV circular dichroism. Typical CD spectra at 20°C are shown in Fig. 3 A. Changing the temperature between 20 and 90°C did not affect the spectral profiles for LamA in solution and in the adsorbed state. LamA free in solution exhibits a broad negative peak at 217 nm and a characteristic positive absorption band starting from ~207 nm that indicate predominantly  $\beta$ -structures (sheets and turns) and negligible contribution from  $\alpha$ -helices. Small differences were observed in the spectrum of LamA adsorbed on Teflon, which according to data analysis were interpreted in terms of an increase of the helical and unstructured domains (Table 1). Adsorption on the silica nanoparticles did not lead to significant changes in the secondary structure of LamA.

### Steady-state fluorescence spectroscopy

On excitation at 300 nm the emission of the tryptophans dominates the fluorescence spectra. LamA in solution shows a strong intensity band at 335 nm (Fig. 3 B), which is char-

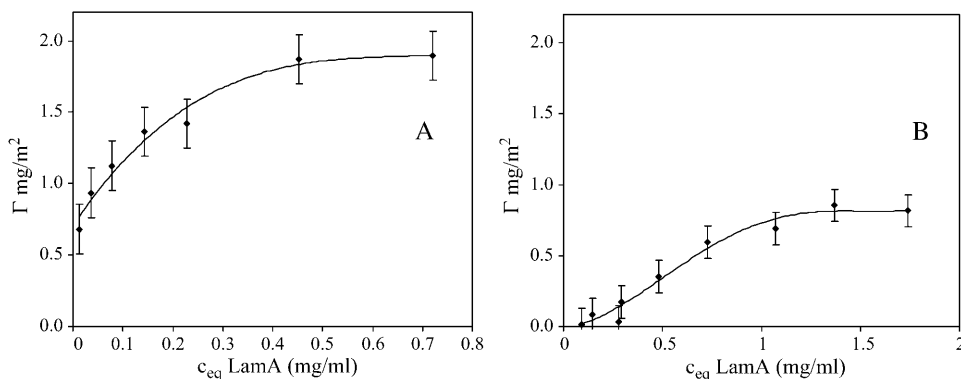


FIGURE 1 Adsorption isotherms for LamA on negatively charged (A) hydrophobic Teflon and (B) hydrophilic silica particles in sodium phosphate 0.01 M and pH 7.0.

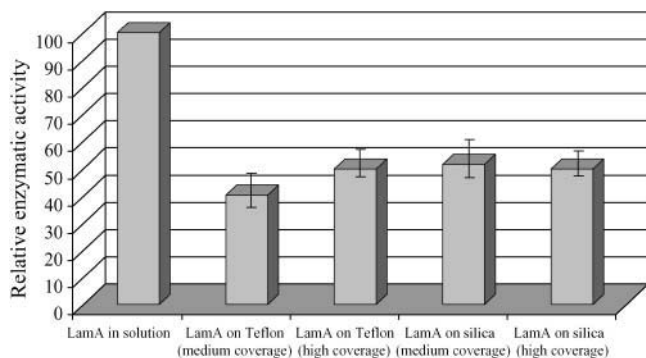


FIGURE 2 Relative specific enzymatic activity of LamA free in solution and adsorbed at medium and maximum surface coverage on Teflon and silica particles. The activity was measured on 5 mg/ml laminarin substrate concentration for 10 min at 90°C in 0.01 M sodium phosphate at pH 7.0.

acteristic of proteins that efficiently shield their tryptophans from the polar solvent and yet, some of them are partially but not completely exposed (Lakowicz, 1999). LamA adsorbed on Teflon shows an emission maximum at 339 nm with a twofold intensity increase as compared to the spectrum of LamA in solution (for the same enzyme concentration). LamA adsorbed on silica shows maximum intensity at the same wavelength as LamA in solution with slightly increased intensity. Comparison of the fluorescence emission spectra of LamA at different temperatures between 20 and 90°C showed a gradual decrease of the fluorescence quantum yield proportionally for LamA in solution and in the adsorbed state whereas the emission maxima were the same.

### Time-resolved fluorescence and anisotropy decay

Fig. 4 A shows the picosecond-resolved fluorescence transients of LamA, which were best fitted by a five-component exponential decay (Table 2) (Beechem, 1992). The decay of LamA in the adsorbed state (*curves b* and *c*) relaxes at longer lifetimes as compared to LamA in solution (*curve a*), which implies less tryptophan quenching. This is also illustrated in the calculated average fluorescence lifetimes  $\langle\tau\rangle$ . Clearly, in the case of LamA adsorbed on Teflon, the tryptophans are significantly less quenched (7.85

ns) as compared to those of LamA in solution or adsorbed on silica (average fluorescence lifetimes 2.13 and 2.22 ns, respectively). This is in line with the differences observed in the intensity of the steady-state fluorescence measurements (Fig. 3 B).

The anisotropy decays as a result of excitation transfer and fluorophore rotation (the tryptophans rotate individually or globally as part of the protein). In each sample the excited state is depopulated by a different mechanism that shows conformation differences (Fig. 4 B). The decays were best fitted by two discrete exponential components (Table 2) (Lakowicz, 1999). The preexponential factor  $\beta_1$  (0.014) of the shorter subnanosecond rotational correlation time,  $\phi_1$ , shows that the tryptophans of LamA adsorbed on Teflon are more constrained and rotate slower around the chemical bond attaching them to the enzyme backbone as compared to the rotation of the indole groups of LamA in solution and adsorbed on silica (0.038 and 0.041, respectively), owing to interactions with neighboring residues or spatial hindrance limitations.

Analysis of the anisotropy decay also gave information on the overall tumbling motion of the enzyme. Inspection of the longer rotational correlation times shows that LamA in the adsorbed state rotates slower (i.e., 85.3 and 115.5 ns for LamA adsorbed on Teflon and silica, respectively) as compared to LamA in solution (18.9 ns). This is not surprising as the tumbling of adsorbed LamA depends on the motion of the particle that carries the macromolecule. The timescale of rotation also shows that LamA is immobilized on the particle. The size of LamA in solution can be calculated from the rotational correlation time,  $\phi_2$ , using the Stokes-Einstein equation ( $\phi = 4\pi R_h^3 \eta / 3kT$ ; where  $\eta$  is the viscosity of the medium,  $k$  is the Boltzmann constant, and  $T$  is the absolute temperature). The hydrodynamic radius,  $R_h$ , was found to be 2.63 nm, which is in excellent agreement with the size of LamA calculated from molecular modeling if the hydration layer is taken into account.

### Differential scanning calorimetry measurements

Working with the hyperthermophilic LamA raised difficulties in operating standard DSC instruments because heat-induced

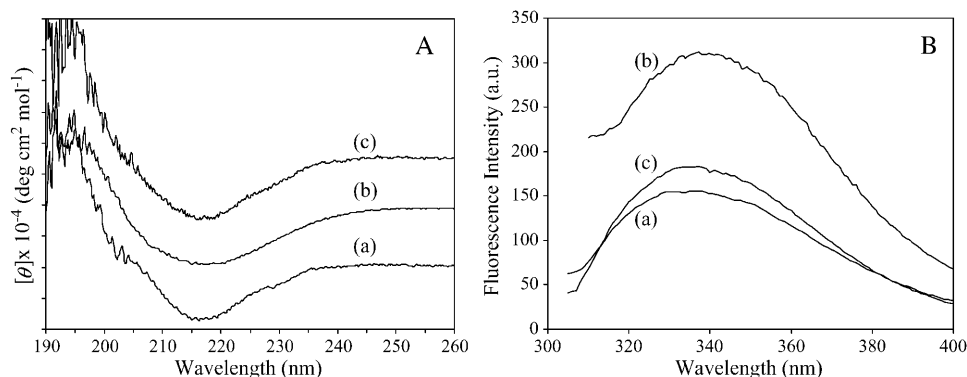


FIGURE 3 Typical far-UV CD (A) and fluorescence emission spectra obtained on excitation at 300 nm (B) of LamA (*a*) in solution and adsorbed on (*b*) Teflon latex, and (*c*) silica nanoparticles (CD spectra were shifted for comparison).

**TABLE 1** Secondary structure of LamA in 0.01 M sodium phosphate at pH 7.0 and in the adsorbed state as calculated from CD spectra using the program CONTIN

Sample	$\alpha$ -helix (%)	$\beta$ -sheet (%)	$\beta$ -turn (%)	Unknown (%)
LamA in solution	0.5 $\pm$ 0.3	74.5 $\pm$ 2.5	21.0 $\pm$ 2.0	4.0 $\pm$ 2.2
LamA on Teflon	15.0 $\pm$ 0.9	47.0 $\pm$ 1.7	16.0 $\pm$ 1.2	23.0 $\pm$ 1.9
LamA on silica	1.0 $\pm$ 0.4	68.0 $\pm$ 1.7	20.5 $\pm$ 1.3	10.5 $\pm$ 1.6

transitions often lay outside the scanning temperature range of the calorimeter. In this work the denaturation of LamA was recorded with a specially constructed calorimeter. In Fig. 5, the DSC thermograms of LamA in solution and in the adsorbed state are presented in the same graph for comparison. Heating LamA resulted in one single calorimetric transition peak. From this peak the temperature of denaturation,  $T_d$ , was determined and the enthalpy,  $\Delta H_{N-D}$ , for the transition between native,  $N$ , and denatured state,  $D$ , was calculated from the peak area using thermodynamic considerations and the formulation of Privalov (Privalov and Gill, 1988). From the results summarized in Table 3, the most important outcome is that adsorption offers further stabilization of LamA requiring higher and more extreme temperatures for denaturation as compared to the enzyme in solution. The stabilization gain of the hyperthermophilic LamA adsorbed on Teflon particles resulted in a transition that was recorded at 133°C. This is 24°C higher than the denaturation temperature of LamA free in solution (i.e., 109°C) at the same experimental conditions. LamA adsorbed on the silica surface was denatured at 116°C, which also points to increased stabilization. Notably, the contribution of the hydrophilic surface to the heat resilience of LamA is less than that of the enzyme in contact with the hydrophobic surface of Teflon.

## DISCUSSION

The conformational characteristics of LamA were studied at the solid/liquid interface. From the thermodynamic point of view, protein adsorption at constant temperature and pressure is determined by the change in Gibbs energy, which

depends on the enthalpy and the entropy of adsorption (Norde, 2000). In the case of LamA, changes in the enthalpy involve repulsive Coulombic interactions and attractive van der Waals forces between protein and interface. Entropic contributions to the Gibbs energy of adsorption originate from hydrophobic dehydration (i.e., displacement of the highly ordered water molecules from hydrophobic surfaces upon adsorption). As the spectroscopic data showed only slight structural rearrangements upon adsorption, changes in the conformational entropy of LamA are very small and, hence, do not significantly contribute to the entropy of adsorption.

From the adsorption isotherms it was shown that LamA was readily adsorbed on both types of negatively charged surfaces opposing repulsive electrostatic interactions. The adsorption of LamA on Teflon is typical of the propensity that proteins have to adsorb on apolar surfaces, even under conditions of electrostatic repulsion (Norde and Anusiem, 1992). However, when a polar surface is involved, “hard” proteins, which denote that structural integrity is maintained upon adsorption, may adsorb only under conditions of electrostatic attraction (Norde and Anusiem, 1992; Shirahama et al., 1990; Norde et al., 1991). Thermodynamically unstable, “soft” proteins adsorb under electrostatically adverse conditions with a subsequent loss of structure. Surprisingly, LamA adsorbed on the polar surface of silica under repulsive electrostatic conditions and yet, maintained its native structural characteristics and biological functioning in the adsorbed state. LamA behaved as a “hard” protein but deviates from the classical definition used up to date. The driving force of LamA’s adsorption on silica is not clear. It might be due to favorable interactions between positively charged groups on the surface of the enzyme (which overall is negatively charged at pH 7.0) and the negatively charged silica surface together with favorable van der Waals interactions.

Examination of the adsorption isotherm profiles provided insight into the adsorption process. A very important aspect of the appraisal is that the initial part of the adsorption isotherm of LamA on silica diverges from the  $\Gamma$ -axis. This indicates a low affinity of LamA for the hydrophilic surface

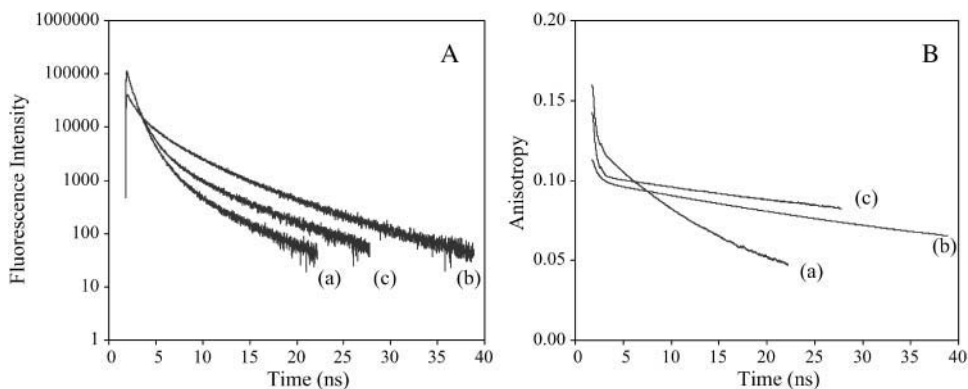


**FIGURE 4** Time-resolved fluorescence emission (A) and anisotropy (B) of LamA (a) in solution and adsorbed on (b) Teflon and (c) silica particles.

**TABLE 2** Calculated parameters from the time-resolved fluorescence and anisotropy decay of LamA in solution and in the adsorbed state, in 0.01 M sodium phosphate at pH 7.0

Sample	Fluorescence										Anisotropy			
	$\alpha_1$	$\tau_1$	$\alpha_2$	$\tau_2$	$\alpha_3$	$\tau_3$	$\alpha_4$	$\tau_4$	$\alpha_5$	$\tau_5$	$\beta_1$	$\phi_1$	$\beta_2$	$\phi_2$
LamA in solution	0.0437	0.028	0.0377	0.233	0.0419	0.612	0.0123	1.463	0.0008	5.521	0.038	0.26	0.122	18.90
LamA on Teflon	0.0076	0.147	0.0138	0.601	0.0080	2.065	0.0044	5.298	0.0004	12.522	0.014	0.50	0.099	85.28
LamA on silica	0.0552	0.026	0.0496	0.328	0.0297	0.940	0.0033	2.880	0.0009	7.607	0.041	0.31	0.102	115.45

Standard errors for the calculation of the decay components were between 5 and 10%.

possibly owing to the electrostatic repulsions. Moreover, the S-shaped isotherm suggests a cooperative adsorption mechanism employed by LamA to overcome the low affinity for the surface: the first molecules of LamA arriving at the interface promote further adsorption by facilitating the approach of more enzyme molecules to the surface. A similar adsorption behavior has been previously observed in another adsorption system (Norde and Zoungrana, 1998). Thus, even though electrostatic repulsions oppose adsorption, binding of the first LamA molecule facilitates adsorption of more enzyme molecules. This can result from attractive protein-protein interactions, which are likely to involve hydrophobic patches of the protein, at the silica surface. Furthermore, we cannot exclude the possibility of changes of the silica surface that would favor further adsorption of LamA. Although we consider the surface of the sorbent as inert this is not completely true. As a result of charge regulation the surface of silica may become less negative or, locally, even positive, upon adsorption of the negatively charged LamA molecules. It has been reported and predicted theoretically that adsorption of a charged species on a like-charged surface induces opposite charges to the surface to meet electroneutrality conditions (Bremer, et al., 2004). Accordingly, adsorption of the first LamA

molecule could render the adjoining silica surface more suitable for further adsorption. Notably, the initial part of the adsorption isotherm is steeper in the case of adsorption on Teflon particles indicating higher affinity of LamA for the hydrophobic surface. The extent of adsorption as reflected in the plateau values also evidences the significance of hydrophobic interactions in the adsorption process.

Application of the principles of interfacial thermodynamics shows that, at the conditions employed, the electrical double layer adjacent to the charged surfaces of the sorbent has a thickness of  $\sim 1.5$  nm. This layer exerts an orientational effect on small proteins so that they are preferentially directed toward the sorbent surface according to their electric dipole (Norde, 1995). This is not the case for LamA because the protein's dimensions exceed the size of the double layer and, hence, is only partly immersed in it upon adsorption. A random orientation of LamA adsorbed on the surface should then be concluded. LamA remains active on both types of surfaces, with decreased activity not attributed to structural changes (as shown from spectroscopic data and from the similarity of the  $K_m$  values for LamA in solution and in the adsorbed state). Therefore, it is reasonable to attribute the activity loss to random orientation of the enzyme at the interface (Fig. 6). A fraction of LamA adsorbs with the cleft oriented toward the surface whereas other molecules expose their active center to the solution where it is accessible for the substrate. Furthermore, in those cases where the enzyme molecules deposit on the surface in an end-on orientation they may subsequently tumble into a side-on configuration in an attempt to optimize contact with the sorbent surface (unless the sorbent surface is tightly packed with protein molecules and, hence, such a shift is not possible due to steric reasons).

Using the specially designed Teflon particles and the silica nanoparticles allowed investigation of the enzyme's structural features in the adsorbed state by standard spectroscopic

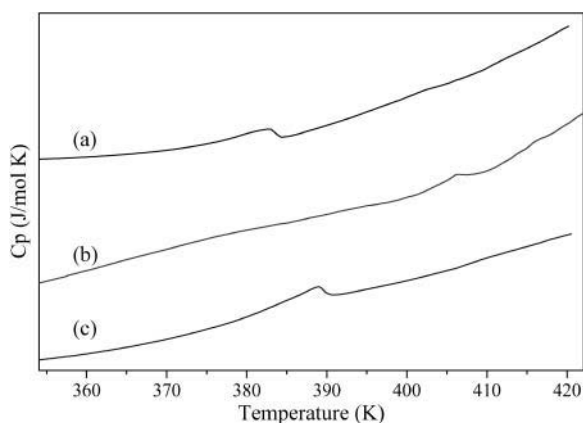


FIGURE 5 Calorimetric studies of the heat-induced denaturation of LamA in 0.01 M sodium phosphate at pH 7.0 (a) in solution and adsorbed on (b) Teflon and (c) silica, measured by DSC (graphs were shifted for comparison).

**TABLE 3** Calorimetric data for the thermal denaturation of LamA in 0.01 M sodium phosphate buffer at pH 7.0 as measured by DSC

Sample	$T_d$ (°C)	$\Delta H_{N-D}$ (kJ mol <sup>-1</sup> )
LamA in solution	109.1 $\pm$ 0.7	407 $\pm$ 9
LamA adsorbed on Teflon	133.0 $\pm$ 1.1	294 $\pm$ 15
LamA adsorbed on silica	115.7 $\pm$ 1.9	389 $\pm$ 13

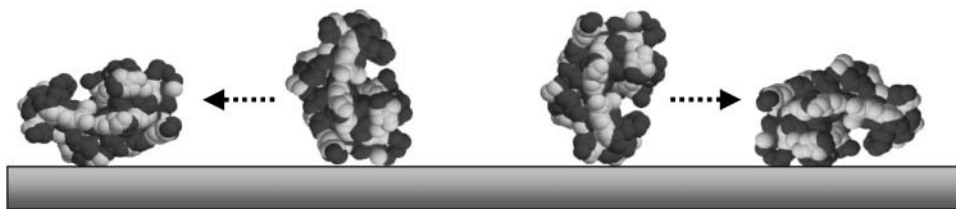


FIGURE 6 The adsorption model schematically. In the graphic display of LamA (created with Rasmol) the dark- and light-shaded balls represent hydrophobic and polar amino acids, respectively. The enzymatic cleft may also be seen. As the protein molecules do not deposit in a preferred orientation but, rather, randomly (whereafter reorienta-

tion of end-on adsorbed molecules into a side-on mode may occur), the active sites of about half of the adsorbed enzyme population is accessible for the substrate.

techniques without the assumptions used in traditional studies. In the case of adsorption on Teflon, analysis of the CD spectroscopic data revealed a slightly distorted secondary structure of LamA in the adsorbed state featuring a decrease of the  $\beta$ -sheets and turns. Changes in the tertiary structure of LamA adsorbed on Teflon were demonstrated by fluorescence emission spectroscopy. The small red shift observed ( $\sim 4$  nm) as compared to LamA in solution implies slightly more exposed tryptophan(s) to water. The intensity increase is possibly due to weaker interactions of the tryptophans with neighboring quenching amino acids (e.g., cysteine, tyrosine, glutamine, etc.) as compared to those in the native conformation (Chen and Barkley, 1998). From both CD and steady-state fluorescence, the spectral differences of LamA in solution and adsorbed on silica nanoparticles are negligible, suggesting similarity of the secondary and tertiary structures.

More information about the conformational characteristics of LamA is obtained from the shape of the time-resolved fluorescence and anisotropy decays (Lakowicz, 1999; Eftink, 1991; Steiner, 1991). The fact that LamA adsorbed on Teflon shows a longer relaxation time upon fluorescence excitation suggests less tryptophan quenching. This is in line with the findings from the steady-state fluorescence measurements. Moreover, the anisotropy decay of LamA on Teflon documents a slight decrease in the global conformational flexibility of the enzyme and a more restricted rotation of the tryptophans in the adsorbed state. Based on these results we can conclude that LamA adsorbed on Teflon undergoes a minor structural distortion. Nevertheless, it remains folded and enzymatically active upon association with both types of particles. This implies that the region around the active center is extremely stable irrespective of possible changes in other parts of the enzyme. These observations evidence an efficient stabilization mechanism that hierarchically preserves the structure of the enzymatic cleft.

Furthermore, monitoring temperature-induced structural changes of LamA in the adsorbed state gave information on the enzyme-surface interactions and its conformational stability. It was shown that the adsorption-induced structural changes in LamA did not lead to heat destabilization. Actually, the opposite was observed: the slightly changed conformation of LamA in the adsorbed state resulted in increased heat stability. The stabilization effect acquired

from interaction of LamA with Teflon reached  $133^\circ\text{C}$ , which is the most extreme experimentally determined denaturation temperature ever reported for a protein. The value of the enthalpy change,  $\Delta H_{\text{N-D}}$ , associated with the heat denaturation is a measure of the intramolecular interactions lost upon denaturation (Privalov, 1979). Comparison of the thermodynamic data for LamA in solution and adsorbed on silica shows that the  $\Delta H_{\text{N-D}}$  is almost the same. However,  $\Delta H_{\text{N-D}}$  for LamA adsorbed on hydrophobic Teflon particles is smaller suggesting that denaturation involved the disruption of fewer intramolecular bonds contributing to the structural coherence. These findings show that even though LamA has undergone more notable structural changes, adsorption on Teflon resulted in a more heat-stable state.

With this study we showed that LamA undergoes minor changes in its secondary and tertiary structure upon adsorption on hydrophobic Teflon and hydrophilic silica particles; however, this did not lead to annihilation of biological functioning. Moreover, the adsorption-induced structural distortion did not result in a less heat-stable form. On the contrary, LamA acquired further stabilization upon interaction with the surfaces. It is suggested that the structural changes observed upon adsorption probably belong to structurally less-constrained domains of the protein. The active site is very stable and, hence, not susceptible to adsorption-induced structural distortions even at high temperatures. This work also suggests that among other mechanisms, nature employs adsorption to preserve life at extreme environmental conditions. Apart from the internal structural features that predominantly assure conformational stability, the extracellular hyperthermophilic LamA may use adsorption as an essential complementary mode to maintain biological functionality at high temperatures. The enzyme may adsorb on the surface of rocks and sediments in the neighborhood of the microorganism's colony to resist abrupt changes in temperature without loss of activity. Moreover, the fact that adsorption stabilizes proteins up to  $133^\circ\text{C}$  raises questions on the sterilization efficiency of the commonly used pressurized autoclaving devices that operate up to  $\sim 120^\circ\text{C}$ .

We thank Dr. J. van Lieshout for assistance with the preparation of the enzyme. We kindly acknowledge Prof. A.J.W.G. Visser and Dr. N. Visser

for helpful discussions with the interpretation of the time-resolved fluorescence experiments. The authors are also grateful to L. Meublant from SETARAM (Caluire, France) for providing access to the calorimeter and to Dr. D. Levý from Dupont de Nemours for granting the Teflon particles. We also acknowledge anonymous reviewers for useful comments.

This research was supported by an individual Marie Curie Fellowship of the European Community program "Improving Human Research Potential and the Socio-Economic Knowledge Base" under contract no. HPMF-CT-1999-00210 (to S.K.).

## REFERENCES

- Beechem, J. M. 1992. Global analysis of biochemical and biophysical data. *Methods Enzymol.* 210:37–54.
- Bowers, L. D., and P. W. Carr. 1980. Immobilized enzymes in analytical chemistry. *Adv. Biochem. Eng.* 15:89–129.
- Bradford, M. M. 1976. A rapid and sensitive method for the quantitation of microgram quantities of protein utilizing the principle of protein-dye binding. *Anal. Biochem.* 72:248–254.
- Bremer, M. G. E. G., J. Duval, W. Norde, and J. Lyklema. 2005. Electrostatic interactions between immunoglobulin (IgG) molecules and a charged sorbent. *Colloids. Surf. A.* 250:29–42.
- Brown, J. R., and W. F. Doolittle. 1997. Archaea and the prokaryote-to-eukaryote transition. *Microbiol. Mol. Biol. Rev.* 61:456–502.
- Chen, Y., and M. D. Barkley. 1998. Toward understanding tryptophan fluorescence in proteins. *Biochemistry.* 37:9976–9982.
- Cherry, J. R., M. H. Lamsa, P. Schneider, J. Vind, A. Svendsen, A. Jones, and A. H. Pedersen. 1999. Direct evolution of a fungal peroxidase. *Nat. Biotechnol.* 17:379–384.
- Combet, C., M. Jambon, G. Deleage, and C. Geourjon. 2002. Geno3D: automatic comparative molecular modelling of protein. *Bioinformatics.* 18:213–214.
- Digris, A. V., V. V. Skakoun, E. G. Novikov, A. van Hoek, A. Claiborne, and A. J. W. G. Visser. 1999. Thermal stability of a flavoprotein assessed from associative analysis of polarized time-resolved fluorescence spectroscopy. *Eur. Biophys. J.* 28:526–531.
- Driskill, L. E., M. W. Bauer, and R. M. Kelly. 1999. Synergistic interactions among  $\beta$ -laminarinase,  $\beta$ -1,4-glucanase, and  $\beta$ -glucosidase from the hyperthermophilic archaeon *Pyrococcus furiosus* during hydrolysis of  $\beta$ -1,4-,  $\beta$ -1,3-, and mixed-linked polysaccharides. *Biotechnol. Bioeng.* 66:51–60.
- Eftink, M. R. 1991. Fluorescence techniques for studying protein structure. *Method. Biochem. Anal.* 35:127–205.
- Greenfield, N. J. 1996. Methods to estimate the conformation of proteins and polypeptides from circular dichroism data. *Anal. Biochem.* 235:1–10.
- Gueguen, Y., W. G. B. Voorhorst, J. van der Oost, and W. M. de Vos. 1997. Molecular and biochemical characterization of an endo- $\beta$ -1,3-glucanase of the hyperthermophilic archaeon *Pyrococcus furiosus*. *J. Biol. Chem.* 272:31258–31264.
- Hahn, M., J. Pons, A. Planas, E. Querol, and U. Heinemann. 1995. Crystal structure of *Bacillus licheniformis* 1,3–1,4- $\beta$ -D-glucan 4-glucanohydrolase at 1.8 Å resolution. *FEBS Lett.* 374:221–224.
- Lakowicz, J. R. 1999. Principles of Fluorescence Spectroscopy, 2nd Ed. Kluwer Academic/Plenum Publishers, New York.
- Lehmann, M., L. Pasamontes, S. F. Lassen, and M. Wyss. 2000. The consensus concept for thermostability engineering of proteins. *Biochim. Biophys. Acta.* 1543:408–415.
- Miller, G. L. 1959. Dinitrosalicylic acid reagent for determination of reducing sugar. *Anal. Chem.* 31:426–428.
- Norde, W. 1995. Adsorption of proteins at solid-liquid interfaces. *Cells Mater.* 5:97–112.
- Norde, W. 2000. Proteins at solid interfaces. In *Physical Chemistry of Biological Interfaces*. A. Baszkin, and W. Norde, editors. Marcel Dekker, New York. 115–135.
- Norde, W., and A. C. I. Anusiem. 1992. Adsorption, desorption and re-adsorption of proteins on solid surfaces. *Colloids Surf.* 66:73–80.
- Norde, W., and T. Zoungrana. 1998. Surface-induced changes in the structure and activity of enzymes physically immobilized at solid/liquid interfaces. *Biotechnol. Appl. Biochem.* 28:133–143.
- Norde, W., T. Arai, and H. Shirahama. 1991. Protein adsorption in model systems. *Biofouling.* 4:37–51.
- Novikov, E. G., A. van Hoek, A. J. W. G. Visser, and J. W. Hofstraat. 1999. Linear algorithms for stretched exponential decay analysis. *Opt. Commun.* 166:189–198.
- Privalov, P. L. 1979. Stability of proteins. Small globular proteins. *Adv. Protein Chem.* 33:167–241.
- Privalov, P. L., and S. J. Gill. 1988. Stability of protein structure and hydrophobic interaction. *Adv. Protein Chem.* 39:191–234.
- Provencher, S. W., and J. Glöckner. 1981. Estimation of globular protein secondary structure from circular-dichroism. *Biochemistry.* 20:33–37.
- Rink, R., M. Fennema, M. Smids, U. Dehmel, and D. B. Janssen. 1997. Primary structure and catalytic mechanism of the epoxide hydrolase from *Agrobacterium radiobacter* AD1. *J. Biol. Chem.* 272:14650–14657.
- Rothschild, L. J., and R. L. Mancinelli. 2001. Life in extreme environments. *Nature.* 409:1092–1101.
- Scouten, W. H. 1983. Solid Phase Biochemistry-Analytical and Synthetic Aspects. John Wiley & Sons, New York.
- Shirahama, H., J. Lyklema, and W. Norde. 1990. Comparative protein adsorption in model systems. *J. Coll. Interface Sci.* 139:177–187.
- Steiner, R. F. 1991. Fluorescence anisotropy: theory and applications. In *Topics in Fluorescence Spectroscopy*, Vol. 2. J. R. Lakowicz, editor. Plenum Press, New York. 1–52.
- Studier, F. W., A. H. Rosenberg, J. J. Dunn, and J. W. Dubendorff. 1990. Use of T7 RNA polymerase to direct expression of cloned genes. *Methods Enzymol.* 185:60–89.
- van den Berg, P. A. W., A. van Hoek, C. D. Walentas, R. N. Perham, and A. J. W. G. Visser. 1998. Flavin fluorescence dynamics and photo-induced electron transfer in *Escherichia coli* glutathione reductase. *Biophys. J.* 74:2046–2058.
- Venyaminov, S. Yu., I. A. Baikov, Z. M. Shen, C. S. Wu, and J. T. Yang. 1993. Circular dichroic analysis of denatured proteins: inclusion of denatured proteins in the reference set. *Anal. Biochem.* 214:17–24.
- Visser, A. J. W. G., P. A. W. van den Berg, N. V. Visser, A. van Hoek, H. A. van den Burg, D. Parsonage, and A. Claiborne. 1998. Time-resolved fluorescence of flavin adenine dinucleotide in wild-type and mutant NADH peroxidase. Elucidation of quenching sites and discovery of a new fluorescence depolarization mechanism. *J. Phys. Chem.* 102:10431–10439.